Orbital Ordering in e_g Orbital Systems: Ground States and Thermodynamics of the 120° Model

Andre van Rynbach,[1] Synge Todo,[2,3] and Simon Trebst[4]

[1]*Physics Department, University of California, Santa Barbara, California 93106, USA*
[2]*Department of Applied Physics, University of Tokyo, Tokyo 113-8656, Japan*
[3]*CREST, Japan Science and Technology Agency, Kawaguchi 332-0012, Japan*
[4]*Microsoft Research, Station Q, University of California, Santa Barbara, California 93106, USA*

Orbital degrees of freedom shape many of the properties of a wide class of Mott insulating, transition metal oxides with partially filled $3d$ shells. Here we study orbital ordering transitions in systems where a single electron occupies the e_g orbital doublet and the spatially highly anisotropic orbital interactions can be captured by an orbital-only model, often called the 120° model. Our analysis of both the classical and quantum limits of this model in an extended parameter space shows that the 120° model is in close proximity to several $T = 0$ phase transitions and various competing ordered phases. We characterize the orbital order of these nearby phases and their associated thermal phase transitions by extensive numerical simulations and perturbative arguments.

Mott insulating transition metal oxides with partially filled $3d$ shells—such as the manganites—exhibit rich phase diagrams with many competing orders, indicating a nontrivial interplay of spin, charge, and orbital degrees of freedom [1]. A prominent example of a material exhibiting *orbital order* is the extensively studied LaMnO$_3$ [2]. The crystal field in this perovskite material splits the five d orbitals into three t_{2g} orbitals occupied by three electrons, and an e_g doublet sharing a single electron. This partially filled e_g doublet then gives rise to an additional orbital degree of freedom indicating which of the two orbitals is occupied. The exchanges between these orbital degrees of freedom—arising from Jahn-Teller distortions or Kugel-Khomskii-type superexchange—are oftentimes described by orbital-only models which neglect the spin degrees of freedom. The latter is justified in situations where the energy scales of spin and orbital interactions are well separated; i.e., orbital interactions correspond to temperature scales where the spins are still largely disordered or in a situation where the spins are effectively frozen out (e.g., by a magnetic field). Expressing the e_g orbital degree of freedom by a two-component pseudospin $\mathbf{T} = (T^z, T^x)$, where $T^z = \pm 1$ correspond to occupation of the $|3z^2 - r^2\rangle$ and $|x^2 - y^2\rangle$ orbitals, the highly anisotropic interactions between them are captured by the so-called 120° model [3] on a cubic lattice

$$
H_{120} = - \sum_{i, \gamma=x,y} \frac{1}{4} [J_z T_i^z T_{i+\gamma}^z + 3J_x T_i^x T_{i+\gamma}^x
$$
$$
\pm \sqrt{3} J_{\text{mix}} (T_i^z T_{i+\gamma}^x + T_i^x T_{i+\gamma}^z)] - \sum_i J_z T_i^z T_{i+z}^z, \quad (1)
$$

where the $\pm$ sign for the "mixing" term enters for coupling along the x and y directions, respectively [4]. If the

orbital exchange is primarily mediated through Jahn-Teller distortions, this model is commonly considered in its classical limit, where the pseudospins $\mathbf{T}$ are $O(2)$ spins. If, on the other hand, the orbital exchange arises primarily from a Kugel-Khomskii-type superexchange [5], this model should be considered in its quantum limit. In the latter case, the pseudospins $\mathbf{T}$ are identified with $SU(2)$ spins; i.e., their components become Pauli matrices $T^{x,z} = \frac{1}{2}\sigma^{x,z}$. The above 120° model has typically been studied at equal coupling $J_x = J_z = J_{\text{mix}}$, for which it exhibits an enhanced rotational symmetry where the symmetry of the cubic lattice under permutations of the x, y, and z axes is reflected in a threefold symmetry in the (T^z, T^x) plane. This becomes apparent when rewriting (1) as $H_{120} = -J\sum_{i, \gamma=x,y,z} (\boldsymbol{\tau}_i \cdot \mathbf{e}^\gamma)(\boldsymbol{\tau}_{i+\gamma} \cdot \mathbf{e}^\gamma)$ where the $\mathbf{e}^\gamma$ are unit vectors in the x, y, z directions and the $\boldsymbol{\tau}_i$ are defined as three-component vectors $\boldsymbol{\tau}_i = ([T_i^z + \sqrt{3}T_i^x]/2, [T_i^z - \sqrt{3}T_i^x]/2, T_i^z)$.

While the presence of this enhanced rotational symmetry for equal coupling has greatly benefitted the understanding of the classical model and has led to a rigorous description of its highly degenerate ground-state manifold [6], it has remained elusive to identify the ground states of the quantum model solely based on symmetry arguments. In this Letter, we will take a broader perspective and study the above 120° model away from this symmetric point and explore ground states and thermodynamic properties in an extended two-dimensional parameter space $(J_x/J_z, J_{\text{mix}}/J_z)$, which in experiments should be accessible by changing pressure or adding a small electric field. Our approach reveals that the original 120° model is in close proximity to several $T = 0$ phase transitions and various competing ordered phases. Combining extensive numerical simulations with analytical arguments we describe the

orbital order in these phases for the classical and quantum limits of this extended 120° model, as well as thermal phase transitions associated with these phases and $T = 0$ phase transitions between them.

The classical model.—For the classical 120° model with rotational symmetry, e.g. $J_x = J_z = J_{mix}$, it has long been appreciated that this model exhibits an infinite, but sub-extensive ground-state degeneracy [6], which is split at low temperatures by an order-by-disorder mechanism stabilizing six ordered states [6,7]. Before turning to the question of how these characteristic features change when exploring the model in the extended parameter space, we will briefly recount their origin in the symmetric model. To this end, we label a general state in the orbital subspace by an angle $|\theta\rangle = \cos(\theta/2)|3z^2 - r^2\rangle + \sin(\theta/2)|x^2 - y^2\rangle$, which for the classical model simply describes the orientation of the $O(2)$ pseudospin vector. To identify the degenerate manifold of ground states, we first observe that any polarized state with all pseudospins being aligned along some angle θ^* is a ground state of Hamiltonian (1). Starting from any such state, further ground states can be found [6,7] by reflecting all orbitals in the xy plane about a line at 0°, the xz plane about 120°, or the yz plane about 240°. Remarkably, we find that this ground-state degeneracy remains (partially) unscathed for an extended parameter regime when moving away from the symmetric model on a line described by $0 \leq J_{mix}/J_z \leq 1$ and $J_x = J_z$. What distinguishes states along this line in parameter space, however, is their instability to thermal fluctuations and the entropic selection of low-temperature states. To discuss this order-by-disorder mechanism we calculate the free energy of the low-temperature states by considering a spin-wave approximation of (1) and expanding to second order in small fluctuations $\delta\theta_i = \theta_i - \theta^*$ about an orbitally ordered state with $\theta_i = \theta^*$ at each site. The resulting free energy $F(\theta^*)$ is plotted in Fig. 1 as a function of J_{mix}/J_z. For $J_{mix} \lesssim 0.8J_z$, the ground-state manifold is lifted and four low-temperature states are entropically favored with their free energy being minimized at angles $\theta^* = 0°, 90°, 180°, 270°$. These four states correspond to orbitally ordered states in orbital configurations given by $|0°\rangle = |3z^2 - r^2\rangle$, $|180°\rangle = |x^2 - y^2\rangle$, and $(|3z^2 - r^2\rangle \pm |x^2 - y^2\rangle)/\sqrt{2}$ for the 90° and 270° states, respectively. For $J_{mix} \gtrsim 0.8J_z$ the 90° minima in the free-energy curves

bifurcate and in total form six minima, all of which become exactly equal only for the symmetric model $J_{mix} = J_z$, where the minima are located precisely at angles of $\theta^* = 0°, 60°, 120°, \ldots 300°$. If we further enlarge J_{mix} beyond J_z, this order-by-disorder phenomenon disappears and we instead find that the ground and low-temperature states are *energetically* selected, with the xz or yz planes ordering in alternating orientations of θ_1 and $\theta_1 + 180°$ where θ_1 continuously changes from $\theta_1 \approx 30°$ to $\theta_1 \approx 45°$ with increasing J_{mix}. This transition between entropic and energetic selection occurs exactly at the symmetric point $J_x = J_z = J_{mix}$ of the 120° model and is accompanied by a first-order phase transition at zero temperature, which becomes apparent in a level-crossing of ground-state energies shown in Fig. 3.

We now turn to a discussion of the thermodynamic properties of the classical 120° model, in particular, the thermal ordering transition into the low-temperature states described above. To investigate the latter we have run extensive Monte Carlo simulations of model (1), going well beyond previous numerics for the (diluted) symmetric model [8]. Concentrating on a family of models, where we vary J_{mix}/J_z but keep $J_x = J_z$ fixed, we find a line of *continuous* thermal phase transitions. Figure 2 shows the specific heat $C_v(T)$ at the transition diverging with linear system size L for two members in this family, the symmetric model with $J_{mix} = J_z$ and a "truncated" model where we drop the mixing terms in Hamiltonian (1), i.e., $J_{mix} = 0$. For all models in this family we can capture the transition to the low-temperature ordered states by a single order parameter M (independent of $J_{mix} \leq J_z$). Since in our numerical simulations we do not know *a priori* which one of the three possible ordering planes the system spontaneously selects at the ordering transition, we define the order parameter as the maximum of the xy, xz, and yz plane magnetizations $M = \max(M_{xy}, M_{xz}, M_{yz})$, where the magnetization in the xy plane is given by $M_{xy} = \sum_z |\sum_{x,y} \mathbf{T}_{x,y,z}|$
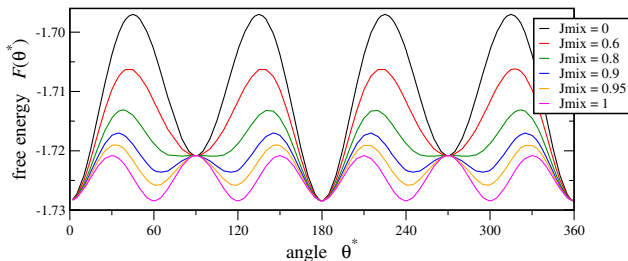

FIG. 1 (color online). Classical free energy $F(\theta^*)$ obtained from a spin-wave analysis of (1) as a function of J_{mix}/J_z for fixed $J_x = J_z$ and $T/J_z = 0.01$.
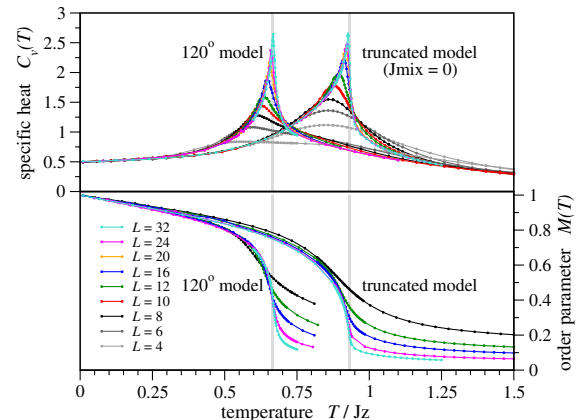

FIG. 2 (color online). Orbital ordering transition in the classical model: Specific heat $C_v(T)$ (upper panel) and order parameter $M(T)$ (lower panel) versus temperature for various system sizes L.

and M_{xz}, M_{yz} are obtained by cyclic permutations of the indices in the sums. As expected this order parameter quickly grows at the transition temperature T_c (see the lower panel of Fig. 2). Despite the relatively large system sizes studied here, finite-size effects still render the identification of the universality class of these transitions somewhat ambiguous, reminiscent of studies of similar models in two spatial dimensions [9]. Tracking the ordering temperature T_c with the strength of the mixing term J_{mix}, as shown in Fig. 3, we find a significant suppression for the symmetric 120° model, for which the transition occurs around $T_c/J_z = 0.677 \pm 0.003$.

The quantum model.—As an inroad into exploring ground states and thermodynamics of the quantum 120° model in an extended $(J_x/J_z, J_{mix}/J_z)$ parameter space around the symmetric point, we first concentrate on a family of models for which the mixing term J_{mix} vanishes but for which we can still vary J_x/J_z. This line in parameter space stands out as it allows for a thorough analysis using quantum Monte Carlo (QMC) simulations, while all other regions in parameter space of nonzero J_{mix} are plagued by the so-called sign problem. Along this line, we first discuss the "truncated" model at equal coupling $J_x = J_z$, for which we have run extensive QMC simulations using an extension of the ALPS looper code [10,11]. Our numerical findings, summarized in Fig. 4, show that this model undergoes a *continuous* thermal phase transition around $T_c/J_z = 0.41 \pm 0.01$ into an orbitally ordered state at low temperatures. In this ordered state all orbitals are found to spontaneously orient in either the $|3z^2 - r^2\rangle$ or $|x^2 - y^2\rangle$ orbital configurations, corresponding to pseudospins pointing in the $\pm T^z$ directions as indicated in Fig. 4(b). This ordered orbital state, which we call the "T^z polarized" state, precisely corresponds to the 0° and 180° states found as low-temperature states in the classical truncated model, indicating that thermal fluctuations and quantum effects favor the same states.

As we vary J_x/J_z away from equal coupling we find that the truncated model above exhibits another peculiarity: it sits right at a first-order transition between different quantum ground states. For $J_x < J_z$ this is the same $\pm T^z$ polarized state found for equal coupling (at finite
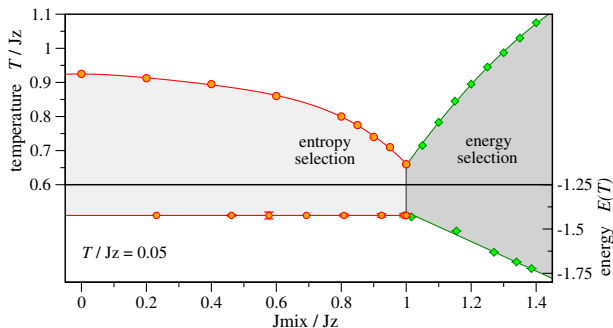
temperature), while for $J_x > J_z$ the pseudospins in any given xy plane point along the $\pm T^x$ directions corresponding to $(|3z^2 - r^2\rangle \pm |x^2 - y^2\rangle)/\sqrt{2}$ orbital configurations (illustrated in the insets of Figs. 5 and 6), but pseudospins in different xy planes do not have to be aligned. This first-order transition is apparent in the level crossing of energies shown in the lower panel of Fig. 5 calculated from both QMC simulations (at temperatures well below the thermal transition) and 2nd order $T = 0$ perturbation expansions around the limits of $J_x = 0$ and $J_x \to \infty$. The good agreement of the two approaches indicates that quantum effects only modestly change the ground states.

Both orbitally ordered phases discussed above exhibit gapped elementary excitations corresponding to a single pseudospin flip, e.g., an "orbital flip" $|3z^2 - r^2\rangle \leftrightarrow |x^2 - y^2\rangle$ in the T^z polarized state. We can directly estimate the excitation gap $\Delta(T)$ of such an "orbiton" excitation in our QMC simulations [11,12] as $\Delta(T) = 2\pi T(\frac{S(0)}{S(2\pi T)} - 1)^{-1/2}$ where $S(\omega)$ is a Fourier transform on an imaginary time correlation function $\sum_r C(r, \tau)$ of the pseudospins. Our results are given in the top panel of Fig. 6. Again we find good quantitative agreement with 3rd order perturbative results (dashed lines) calculated around the limits of $J_x = 0, \infty$. For both orbitally ordered phases, the orbiton gap is suppressed as one approaches the truncated model at equal coupling, where for both phases we measure a gap of $\Delta(J_x = J_z) = (0.34 \pm 0.04)J_z$ (significantly smaller than the estimate $\Delta \approx 0.47 J_z$ from an $1/S$ expansion [13]). As a consequence, the temperature of the thermal phase transition is also significantly suppressed in the vicinity of the truncated model (see Fig. 5).

Having established the nature of the ordered phases for vanishing mixing term, we are now in a position to return
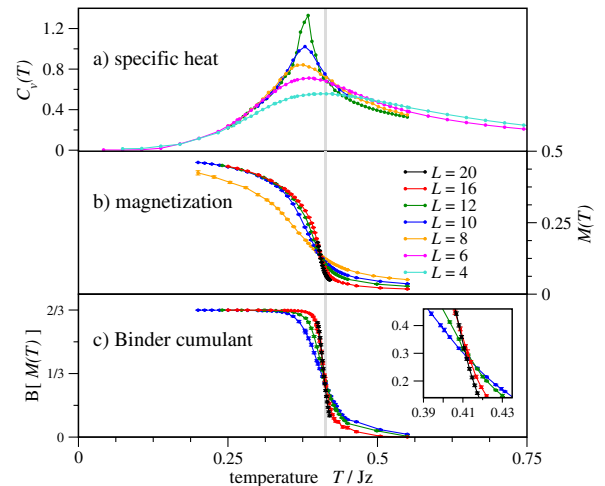

FIG. 4 (color online). Orbital ordering transition in the truncated quantum model: (a) specific heat $C_v(T)$, (b) magnetization $M(T) = |\sum_i T_i^z|$, and (c) Binder cumulant $B[M(T)] = 1 - \langle M(T)^4\rangle/3\langle M(T)^2\rangle^2$. The latter exhibits a crossing point for data of different system sizes L, indicative of a continuous transition [15].

FIG. 3 (color online). Transition temperature (upper panel) and ground-state energy (lower panel) in the classical model for varying J_{mix}. The 120° model corresponds to $J_{mix} = J_z$.
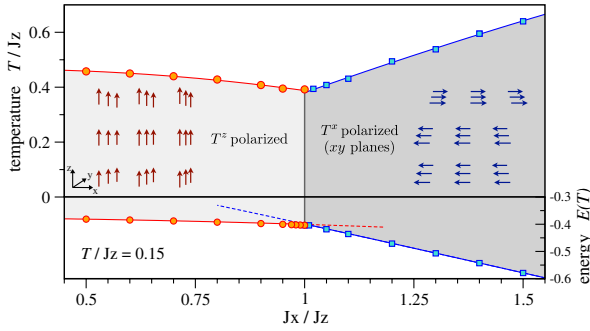
FIG. 5 (color online).   Transition temperature (upper panel) and ground-state energy (lower panel) for the quantum model.

to a discussion of the 120° model in the full (J_x/J_z, J_{mix}/J_z) parameter space. While a small mixing term $J_{mix} \neq 0$ will not affect these gapped phases, a sufficiently large mixing term can close the orbiton gap. For large J_{mix}, a mean-field approximation indicates an "orthogonal" ordered orbital state where the pseudospins are aligned within each xz (or yz) plane, but aligned approximately perpendicular to each other between planes. Assuming that the instability of the polarized phases indeed arises primarily from orbiton condensation (and is not preempted by some other transition), we can map out a phase boundary in parameter space by calculating a $T = 0$ perturbation expansion of the orbiton gap in J_{mix}/J_z. Our results are shown in the lower panel of Fig. 6, where the lines indicate the closing of the orbiton gap when considering 2nd order corrections to the gap values for a given ratio J_x/J_z calculated either from QMC simulations (symbols) or perturbation theory (dashed lines). Interestingly, these phase boundaries intersect the $J_x = J_z$ axis at values of J_{mix}/J_z just above one, the location of the symmetric 120° model. Given that the perturbative results *overestimate* the critical value of J_{mix}/J_z, one might be tempted to conclude that the symmetric model is right at a multicritical point between the three phases. In particular, this would indicate that the
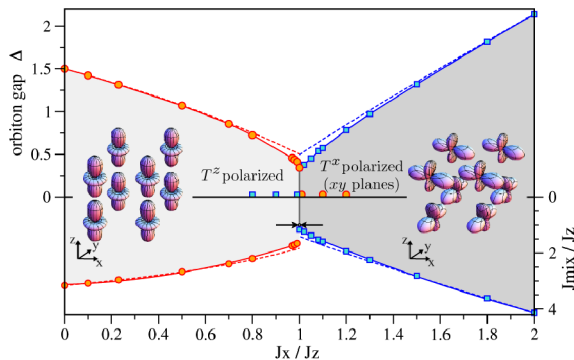
quantum ground states found for the truncated model at $J_{mix}/J_z = 0$ adiabatically connect to the ground states at the symmetric point. However, at the symmetric point the rotational symmetry requires that if the $|3z^2 - r^2\rangle$ ($|x^2 - y^2\rangle$) orbital states (i.e., the $\pm T^z$ polarized states) remain ground states, then also their symmetry related $|3x^2 - r^2\rangle$ ($|y^2 - z^2\rangle$) and $|3y^2 - r^2\rangle$ ($|z^2 - x^2\rangle$) orbital states must become ground states. This leaves us with two possible scenarios to connect the T^x polarized states of the truncated model to the symmetric point. (i) Quantum effects for nonzero J_{mix} have the same effect as thermal fluctuations in the classical model and these states adiabatically turn into a combination of the symmetry required states above (with two more states coming down from higher energies). Some support for this scenario comes from considering a $1/S$ expansion for varying $0 \leq J_{mix}/J_z \leq 1$ (generalizing previous calculations [13,14]), which in linear order gives a zero-point energy that mimics the behavior of the free energy obtained for the classical model in Fig. 1; i.e., two minima at 90° and 270° found in the vicinity of the truncated model bifurcate with increasing J_{mix}/J_z. (ii) The T^x polarized state remains unchanged and brings in four more symmetry related states. Scenario (i) thus selects exactly the same six ordering states at angles 0°, 60°,... as in the classical symmetric model, while for scenario (ii) we get 12 ordering states at angles 0°, 30°, 60°,...330°.

We acknowledge discussions with L. Balents, A. Lauchli, Z. Nussinov, J. van den Brink, and M. Zhitomirsky.

[1] Y. Tokura and N. Nagaosa, Science **288**, 462 (2000).
[2] Y. Murakami *et al.*, Phys. Rev. Lett. **81**, 582 (1998); E. Saitoh *et al.*, Nature (London) **410**, 180 (2001).
[3] For a recent overview see, e.g., J. v. d. Brink, New J. Phys. **6**, 201 (2004) and references therein.
[4] On the cubic lattice we can transform the antiferromagnetic 120° model [3] to a ferromagnetic one through rotations of all pseudospins by an angle π about the T^y axis on one sublattice.
[5] K. I. Kugel and D. I. Khomskii, JETP Lett. **15**, 446 (1972).
[6] M. Biskup *et al.*, Commun. Math. Phys. **255**, 253 (2005).
[7] Z. Nussinov *et al.*, Europhys. Lett. **67**, 990 (2004).
[8] T. Tanaka, M. Matsumoto, and S. Ishihara, Phys. Rev. Lett. **95**, 267204 (2005); T. Tanaka and S. Ishihara, Phys. Rev. B **79**, 035109 (2009).
[9] S. Wenzel, W. Janke, and A. M. Lauchli, Phys. Rev. E **81**, 066702 (2010).
[10] A. F. Albuquerque *et al.*, J. Magn. Magn. Mater. **310**, 1187 (2007).
[11] S. Todo and K. Kato, Phys. Rev. Lett. **87**, 047203 (2001).
[12] S. Todo *et al.*, Phys. Rev. B **64**, 224412 (2001).
[13] K. Kubo, J. Phys. Soc. Jpn. **71**, 1308 (2002).
[14] J. van den Brink *et al.*, Phys. Rev. B **59**, 6795 (1999).
[15] The continuous nature of this transition is further corroborated by the observation of no bimodal histograms of the energy, magnetization or other observables.

FIG. 6 (color online).   Phase diagram of the quantum 120° model: The upper panel shows the orbiton gap of the orbital polarized states as a function of J_x/J_z and $J_{mix} = 0$ obtained from QMC simulations at $T/J_z = 0.15$ (symbols) and 3rd order perturbation theory (dashed lines). The lower panel shows the critical value of J_{mix} at which the orbiton gap closes. The location of the symmetric 120° model is indicated by the arrows.